PPARδ-mediated p21/p27 induction via increased CREB-binding protein nuclear translocation in beraprost-induced antiproliferation of murine aortic smooth muscle cells

Yuh-Mou Sue, Chih-Peng Chung, Heng Lin, Ying Chou, Chih-Yu Jen, Hsiao-Fen Li, Chih-Cheng Chang and Shu-Hui Juan

Am J Physiol Cell Physiol 297:C321-C329, 2009. First published 8 July 2009;
doi:10.1152/ajpcell.00069.2009

You might find this additional info useful...

This article cites 34 articles, 15 of which can be accessed free at:
http://ajpcell.physiology.org/content/297/2/C321.full.html#ref-list-1

This article has been cited by 1 other HighWire hosted articles
The PPAR-RXR Transcriptional Complex in the Vasculature: Energy in the Balance
Jorge Plutzky
Circulation Research, April 14, 2011; 108 (8): 1002-1016.
[Abstract] [Full Text] [PDF]

Updated information and services including high resolution figures, can be found at:
http://ajpcell.physiology.org/content/297/2/C321.full.html

Additional material and information about ***AJP - Cell Physiology*** can be found at:
http://www.the-aps.org/publications/ajpcell

This infomation is current as of May 27, 2011.

AJP - Cell Physiology is dedicated to innovative approaches to the study of cell and molecular physiology. It is published 12 times a year (monthly) by the American Physiological Society, 9650 Rockville Pike, Bethesda MD 20814-3991. Copyright © 2009 by the American Physiological Society. ISSN: 0363-6143, ESSN: 1522-1563. Visit our website at http://www.the-aps.org/.

Downloaded from ajpcell.physiology.org on May 27, 2011

Am J Physiol Cell Physiol 297: C321–C329, 2009;
doi:10.1152/ajpcell.00069.2009.

PPARδ-mediated p21/p27 induction via increased CREB-binding protein nuclear translocation in beraprost-induced antiproliferation of murine aortic smooth muscle cells

Yuh-Mou Sue,[1] Chih-Peng Chung,[2] Heng Lin,[3] Ying Chou,[2] Chih-Yu Jen,[2] Hsiao-Fen Li,[4] Chih-Cheng Chang,[2] and Shu-Hui Juan[2,5]

[1]*Department of Nephrology, Taipei Medical University-Wan Fang Hospital, Taipei;* [2]*Graduate Institute of Medical Sciences, Taipei Medical University, Taipei;* [3]*Institute of Pharmacology and Toxicology, Tzu Chi University, Hualien;* [4]*Graduate Institute of Life Sciences, National Defense Medical Center; and* [5]*Department of Physiology, Taipei Medical University, Taipei, Taiwan*

Submitted 11 February 2009; accepted in final form 24 May 2009

Sue YM, Chung CP, Lin H, Chou Y, Jen CY, Li HF, Chang CC, Juan SH. PPARδ-mediated p21/p27 induction via increased CREB-binding protein nuclear translocation in beraprost-induced antiproliferation of murine aortic smooth muscle cells. *Am J Physiol Cell Physiol* 297: C321–C329, 2009. doi:10.1152/ajpcell.00069.2009.—We previously showed that an increase in the peroxisome proliferator-activated receptor-δ (PPARδ), together with subsequent induction of inducible nitric oxide synthase (iNOS) by beraprost (BPS), inhibits aortic smooth muscle cell proliferation. Herein, we delineated the mechanisms of the antiproliferative effects of BPS through the induction of p21/p27. BPS concentration dependently induced the p21/p27 promoter- and consensus cAMP-responsive element (CRE)-driven luciferase activities, which were significantly suppressed by blocking PPARδ activation. Surprisingly, other than altering the CRE-binding protein (CREB), BPS-mediated PPARδ activation increased nuclear localization of the CREB-binding protein (CBP), a coactivator, which was further confirmed by chromatin immunoprecipitation. Furthermore, novel functional PPAR-responsive elements (PPREs) next to CREs in the rat p21/p27 promoter regions were identified, where PPARδ interacted with CREB through CBP recruitment. BPS-mediated suppression of restenosis in mice with angioplasty was associated with p21/p27 induction. Herein, we demonstrate for the first time that BPS-mediated PPARδ activation enhances transcriptional activation of p21/p27 by increasing CBP nuclear translocation, which contributes to the vasoprotective action of BPS.

cAMP-responsive element; cAMP-responsive element-binding protein; cAMP-responsive element-binding protein-binding protein; antiproliferation

PROSTACYCLIN (PGI_2), synthesized by vascular endothelium and smooth muscle cells (SMCs), acts on vascular tissues to relax smooth muscles and reduce vascular resistance by direct vasodilation (8). Its action is, on the one hand, mediated by binding to a specific G protein-coupled receptor the PGI_2 receptor (IP) thereby activating intracellular signaling pathways (17, 27); but on the other hand, PGI_2 and its stable analog beraprost (BPS) were shown to exert their effects by serving as ligands of peroxisome proliferator-activated receptor δ (PPARδ), a nuclear hormone receptor (23, 27). PPARδ modulates target gene expressions in response to ligand activation after heterodimerization with the retinoid X receptor and binding to peroxisome proliferator-responsive elements (PPREs) of target genes (1, 12). Therefore, PPARδ-mediated modulation of gene transcription by PGI_2 may form the basis for its novel role as a regulator of gene expression (7). Additionally, PPARδ activation was shown to play a beneficial role in preventing atherosclerotic lesions. For instance, a potent and selective PPARδ agonist GW0742X was shown by Graham et al. to reduce atherosclerosis in $LDLR^{-/-}$ mice (5). Furthermore, we previously linked the causal relationship of PPARδ and inducible nitric oxide synthase (iNOS) in reducing neointimal formation of the murine carotid artery with balloon injury (13). Those observations suggest an atheroprotective effect of PPARδ agonists in vivo.

Additionally, BPS was shown to activate endothelial nitric oxide synthase (eNOS) (18) and regulate the cell cycle of vascular SMCs through cAMP signaling by preventing the downregulation of p27 (9). cAMP, a second messenger produced by adenylyl cyclase, activates protein kinase A (PKA) to initiate multiple phosphorylation reactions and thus regulates various functions within cells (13). However, it was recently shown that phosphorylation of the cAMP receptor element-binding protein (CREB) failed to induce transcription at the majority of identified CREB target genes due to the absence of CREB-binding protein (CBP)/p300 occupancy (3, 30, 34). The CBP is a highly regulated mammalian transcriptional coactivator that regulates gene transcription through various activities (4). It is known to enhance gene transcription by linking sequence-specific transcription factors to the RNA polymerase II holoenzyme (16). It also promotes gene transcription by forcing chromatin into conformations that are more accessible to DNA-binding transcription factors through the acetylation of histones (19). Numerous studies have shown that the transcription factor coactivator CBP is involved in inducing numerous genes, such as p53 and p27 (6, 11). Moreover, loss of CBP causes T cell lymphomagenesis synergistically with p27 insufficiency by decreasing gene transcription and increasing protein degradation (11). Despite the evidence that CREB phosphorylation is insufficient for coactivator recruitment and activation of numerous genes in vivo (3), the molecular or signaling pathway involved in CBP recruitment that increases CRE-driven downstream transactivation remains to be characterized.

Cell-cycle progression is mediated by activation of cyclins and cyclin-dependent kinases (CDKs), which act together to initiate progression to the S phase and mitosis from the G1 and G2 phases of the cell cycle, respectively. Cyclin-CDK com-

Address for reprint requests and other correspondence: S.-H. Juan, Graduate Institute of Medical Sciences and Dept. of Physiology, Taipei Medical Univ., 250 Wu-Hsing St., Taipei 110, Taiwan (E-mail: juansh@tmu.edu.tw).

 0363-6143/09 $8.00 Copyright © 2009 the American Physiological Society

Downloaded from ajpcell.physiology.org on May 27, 2011

plexes in cell-cycle progression are regulated by CDK inhibitors (CDKIs), such as p21/Cip1 and p27/Kip1, which prevent abnormal proliferation by blocking their catalytic activities (26). p21 and p27 are believed to inhibit their targets through similar mechanisms due to the high level of homology of their primary structures. Additionally, PGI_2 was shown to inhibit the proliferation of primary arterial SMCs by eliminating CRE-mediated cyclin A gene expression via a G-protein-linked pathway, resulting in the blocking of cell cycle progression from the G1 to the S phase (28). The antiproliferative effect of PGI_2 on cyclin and CDK complex formation was extensively elucidated, whereas the involvement of p21 and p27 in the prevention of restenosis or its underlying molecular mechanisms is still unclear.

We hypothesized that BPS-mediated p21/p27 induction is regulated by an increase in the nuclear translocation of PPARδ and CBP in rat aortic SMCs (RASMCs). Herein, we attempted to unravel the molecular mechanisms of the BPS-mediated increase in nuclear translocation of PPARδ and CBP, thereby increasing CRE/PPRE-driven p21/p27 induction and subsequently the antiproliferative effect of BPS in RASMCs. In addition to the primary culture system, the molecular mechanisms of BPS associated with p21/p27 induction in the preventing neointimal formation in mice with balloon injury of the carotid artery were examined.

MATERIALS AND METHODS

Isolation and primary culture of RASMCs. RASMCs were isolated from the thoracic aorta of male Sprague-Dawley rats (275~325 g) using an explant technique (2). The animal use protocol was reviewed and approved by the Institutional Animal Care and Use Committee. Briefly, after removal of the endothelium and adventitia, the aortic explants were cultured in Dulbecco's modified Eagle's medium (DMEM) and supplemented with 10% fetal bovine serum (FBS) from Invitrogen (Carlsbad, CA), penicillin (100 U/ml), streptomycin (100 μg/ml), and 25 mM HEPES (pH 7.4). After 2 wk, cells that had migrated out of the explants were removed by trypsinization and successively subcultured. The purity and identity of cells were examined by immunostaining using an antibody specific for smooth muscle cell α-actin. Cells from passages 5 to 12 were used for the experiments.

[^{3}H]thymidine incorporation. As previously described (10), cells at a density of 1×10^4 cells/cm^3 were applied to 24-well plates in DMEM plus 10% FBS. After cells had grown to 70%~80% confluence, they were rendered quiescent by incubation for 72 h in DMEM containing 0.04% FBS. BPS was purchased from Cayman (Ann Arbor, MI). Chemicals as indicated or dimethyl sulfoxide (DMSO) in 10% FBS were added to the cells, and the mixture was incubated for 27 h. During the last 4 h of incubation with or without BPS, [^{3}H]thymidine was added at 1 μCi/ml (1 μCi = 37 kBq). The incorporated [^{3}H]thymidine was extracted in 0.2 N NaOH and measured in a liquid scintillation counter.

Constructs of the CRE enhancer and p21/p27 promoter variants and luciferase activity assay. A luciferase reporter plasmid driven by the CRE known to be activated by the recruitment of CREB and CBP, a transcriptional coactivator, was prepared for the assay. In brief, the oligonucleotides with a triple repeat of the CRE obtained from the rat tyrosine hydroxylase enhancer region (TGACGTCAGCCT) (22) and CRE mutant (CTagaactCCCT) were cloned into the *Kpn*I and *Nhe*I sites of the pGL2-promoter vector (Promega, Madison, WI), and respectively, designated pGL2-3CRE and pGL2-3mCRE.

The methods for obtaining the human p21/p27 promoter constructs cloned in the pGL3-promoter vector were described previously (21). Moreover, with in silico analysis using MatInspector Professional software, there was a putative PPRE predicted next to the putative CRE binding site for both rat p21/p27 promoters. The CRE/PPRE fragments spanning −8671 to −8400 of the p21 and −1187 to −950 of the p27 promoters were obtained by polymerase chain reaction (PCR) amplification using rat genomic DNA as the template. The putative CRE/PPRE sequences for the p21 and p27 promoter regions were, respectively, the following:

5′-**CCTGTGCTT**AGGTCA**TTTTCT**GTTCTGTCTTTT
TTCTGGGGTCTCACTTCTCGGGAGTTTGTGTGGAGGTGACTTCTTCTGAAATCT
AGCTGTCCCTGTTTGGGACTCCCCAGTCCTTTTCTGGGAAATGGTGATCTTG-3′

and

5′-**TAGCT**AAGTCA**CCCTGCGGG**GAGTGGGGGTGGGGGGGGATCCCAGGCACCGAG
CCAAGGTTTCCTGGATCTTTCGCCTACCCTCC-3′

(the putative CREs/PPREs are in boldface and underlined, respectively). The boxed nucleotides are their conserved sequences where AGGTCA and AAGTCA are the putative CREs of p21s and p27s, respectively, TGGGAAaTGGTGA is the sense (+) strand for p21PPRE-RXR, and GGATCTtTCGCCT is the antisense (−) strand for p27RXR-PPRE. Sequences of primer pairs with the *Kpn*I or *Bgl*II site at the 5′ ends for amplification of p21/p27 promoter fragments were 5′-TCTGGTACCGGAGCTGAGGCTGG-3′ and 5′-CTCAGATCTAGCTGCTGGAGCTAC-3′ (for the rat p21 promoter) and 5′-CAGGGTACCTTCCTTTTTGAAGCCG-3′ and 5′-GCTAGATCTTTGGAGCCTCAGTGGC-3′ (for the rat p27 promoter). Furthermore, the putative CRE mutants of p21 and p27 were obtained by two rounds of PCR that utilized two flanking primers and internal mutagenic primers. Sequences of the internal mutagenic primers for the CRE and PPRE mutants of p21 and p27 were 5′-GAACAgAAAAAgTTCTAAgCA-3′, 5′-CCCGCAGGGAGTTCTAGCTA-3′ (CRE mutants), 5′-CAAGATCGAACCCTCCCAGAAAAG-3′, and 5′-GGAGGGTAGGCGCCCAACCCAGG-3′ (PPRE mutants) (the mutated sequences are in boldface and underlined), respectively. The wild types and mutants for the putative CRE/PPRE fragments of p21 and p27 were digested with *Kpn*I and *Bgl*II restriction enzymes followed by subcloning into the *Kpn*I-*Bgl*II site of the pGL2-promoter vector, and the resulting constructs were respectively designated pGL2-rp21, -rp21mCRE, -rp21mPPRE, -rp21double mutation (dm), -rp27, -rp27mCRE, -rp27mPPRE, and -rp27dm. The identities of the sequences were confirmed using an ABI PRISM 377 DNA Analysis System (Perkin-Elmer, North Point, Hong Kong).

For the reporter activity assay, cells were seeded in 24-well plates at a density of 1×10^5 cells/well. In brief, RASMCs were transiently transfected with 1.02 μg of plasmid DNA containing 0.02 μg of the Renilla luciferase construct pRL-TK (Promega) to control transfection efficiency, and 1 μg of the pGL3/p21(−2300/+8), p27(−1358/+132), and pGL2-CRE promoter variants using LipofectAMINE

Downloaded from ajpcell.physiology.org on May 27, 2011

2000 (Invitrogen). After transfection for 4 h, the medium was replaced with complete medium and incubation continued for another 20 h. Transfected cells were then treated with drugs for 6 or 12 h as indicated, and cell lysates were collected. Luciferase activities were recorded in a TD-20/20 luminometer (Turner Designs, Sunnyvale, CA) using a dual luciferase assay kit (Promega) according to the manufacturer's instructions. Luciferase activities of the reported plasmids were normalized to luciferase activities of pRL-TK.

PPARδ and CBP siRNA preparation and transient transfection. PPARδ small interfering (si)RNA (AUGAAGGGUGCGUUAUGGCTG) and CBP siRNA (GCUAUGGCCAGAGUUACUAUU) duplexes were chemically synthesized by Ambion (Austin, TX). RASMCs were seeded in a six-well plate and transfected with either 100 pmole of PPARδ siRNA (no. 16708, Ambion), CBP siRNA (no. 16104, Ambion), scrambled control siRNA (no. 4611, Ambion), or GAPDH siRNA (no. 4624, Ambion) in a 100-μl volume with siPORT NeoFX. The efficiency of siRNA silencing was analyzed by Western blotting after transfection for 48 h, followed by BPS treatment for the indicated time periods.

Analysis of gene expression by RT-PCR and Western blot analysis. The method to obtain total RNA for the reverse transcription (RT)-PCR analysis was as described previously (21) with minor modifications. Sequences of the primer pairs for amplification of each gene were 5′-GTGGACAGTGAGCAGTTGA-3′ and 5′-GAGTCTTCAGGCCTCTCAG-3′ (for the p21 gene), 5′-CAGAATCATAAGCCCCTGGA-3′ and 5′-GGGGAACCGTCTGAAACATT-3′ (for the p27 gene), and 5′-CCACCATGGAGAAGGCTGGGGCTCA-3′ and 5′-ATCACGCCACAGTTTCCCGGAGGGG-3′ (for the GAPDH gene). Total RNA, at 5 μg, of extracts from the RASMCs was used. The level of the housekeeping gene GAPDH was analyzed and used to demonstrate the presence of the same amount of total cDNA in each RNA sample. Expression levels of p21/p27 were detected from the same samples using the appropriate primers. Bands separated on 2% agarose gels were visualized and quantified with an electrophoresis image analysis system (Eastman Kodak, Rochester, NY). Antibodies for p21, p27 (BD Biosciences, San Jose, CA), PPARδ (sc-7197), CBP (Santa Cruz, CA), GAPDH (Biogenesis, Kingston, NH), histone H3 (BioVision, Mountain View, CA), and total and phosphorylated CREB (Upstate Biotechnology, Lake Placid, NY) were included in the assay. The cell lysate (50 μg) was electrophoresed on an 8% sodium dodecylsulfate (SDS)-polyacrylamide gel and then transblotted onto a Hybond-P membrane (GE Healthcare). The following procedures were described everywhere.

Electrophoretic mobility shift assay using in vitro translation of the PPARδ protein. Total RNA was prepared from cultures by directly lysing cells in TRIzol buffer (Life Technologies, Gaithersburg, MD), and mRNAs were reversed transcribed into cDNA using oligo-dT and hexamer primers by reverse transcriptase (Invitrogen). After first-strand cDNA synthesis, the cDNA was used as a template and amplified by pairs of primers derived from PPARδ for the RT-PCR. Sequences of the primer pairs for amplification of PPARδ were 5′-TCAGTCATGGAACAGCCACAG-3′ and 5′-GTGCAGCCTTAGTACATGTCC-3′. Rat PPARδ cDNA containing the entire coding sequence was inserted into the T&A cloning vector (RBC Bioscience) with the T7 promoter flanked at the 5′ position, which was then in vitro-translated using the TNT T7 quick-coupled transcription/translation system (Promega). The resulting translated PPARδ was confirmed by Western blot analysis, which was then subjected to electrophoretic mobility shift assay (EMSA) analysis for its binding activity with PPRE oligonucleotides derived from the p21/p27 promoters.

The EMSA was performed as described previously (29) with minor modifications. Sequences of oligonucleotides respectively used CCTTTTCTGGGAAATGGTGATCT and GATCTTTCGCCTACCCTCC for the putative p21 and p27 PPREs. The oligonucleotide was end-labeled with [γ-^{32}P]dATP. The in vitro-translated protein was incubated with 0.1 ng of [^{32}P]DNA for 15 min at room temperature in 25 μl of binding buffer containing 1 μg of poly (dI-dC). For competition with unlabeled oligonucleotides, a 100-fold molar excess of unlabeled oligonucleotides relative to the radiolabeled probe was added to the binding assay. The mixtures were electrophoresed on 5% nondenaturing polyacrylamide gels. Gels were dried and imaged by means of autoradiography.

Immunofluorescence staining. RASMCs were cultured on poly-L-lysine-coated 0.17-mm coverslips for 2~3 days, and cells numbers were counted at 50%~80% confluence. Cells were fixed in 4% formaldehyde for 15 min. Cells were permeabilized with 0.2% Triton and 0.1% Tween 20 in blocking buffer (3% BSA in PBS) for 2 h. Antibodies used for staining included rabbit anti-CBP followed by FITC-labeled goat anti-rabbit immunoglobulin G (IgG) (Jackson Immunoresearch, West Grove, PA). Coverslips were mounted on slides with Vectashield antifade (Vector) diluted 1:1 with PBS, and images were obtained with a DMI 6000B CS laser confocal microscope (Leica) using an HCX PL APO l-blue 63×/1.40–0.60 numerical aperature oil-immersion objective lens for RASMCs. Images were acquired with a CM350 CCD camera (Applied Precision, Issaquah, WA) using TCS SP5 confocal spectral microscope imaging system software (Leica) and processed with Photoshop 7.0 software (Adobe System, San Diego, CA).

Coimmunoprecipitation. CREB, PPARδ, or CBP was immunoprecipitated from 200 μg protein using anti-CREB or anti-PPARδ (sc-7197) antibodies (2 μg) and protein A plus G agarose beads (20 μg). The precipitates were washed five times with lysis buffer and once with PBS. The pellet was then resuspended in sample buffer [50 mM Tris, (pH 6.8), 100 mM bromophenol blue, and 10% glycerol] and incubated at 90°C for 10 min before electrophoresis to release the proteins from the beads.

ChIP assay. A chromatin immunoprecipitation ChIP assay was performed according to the instructions of Upstate Biotechnology (Lake Placid, NY) with minor modifications. Briefly, 6×10^5 cells were cultured in 100-mm dishes and pretreated with or without PPARδ antagonists for 1 h before BPS administration for 4 h. The resulting supernatant was subjected to overnight Coimmunoprecipitation (co-IP) using either anti-CREB, anti-CBP, or anti-PPARδ (sc-7197) antibodies, or the same amount of a nonspecific antibody [mouse monoclonal α-tubulin (α-Tu); Sigma Chemical; St. Louis, MO] as a negative control, followed by incubation with a salmon sperm DNA/protein G agarose slurry (Upstate, Charlottesville, VA) to immobilize the DNA-protein-antibody complex. DNA-protein complexes were then eluted with 200 μl of elution buffer (Tris-EDTA buffer containing 1% SDS) for 30 min, and the cross-links were reversed by overnight incubation at 65°C. DNA was purified using a PCR purification kit (Qiagen, Hilden, Germany). The DNA filtrates were amplified by PCR with primers flanking the promoter of the p21/p27 genes containing the putative CRE and PPRE: p21 forward (5′-GGAGCTGAGGCTGGAGAAGT-3′) and reverse primers (5′-AGCTGCTGGAGCTACTCAGG-3′) and p27 forward (5′-TTCCTTTTTGAAGCCGTCTC-3′) and reverse primers (5′-TTGGAGCCTCAGTGGCTAGT-3′). Additionally, the template was replaced with double-distilled H_2O as a negative internal control. The PCR products were electrophoresed on a 2% agarose gel, and PCR products of the expected sizes of 253 and 219 bp were visualized, quantified using the Image analysis system, and eluted from the agarose gel for sequencing to verify the site of amplification.

Immunohistochemistry of mice with carotid injury. The methods for carotid injury and its subsequent BPS treatment were described previously (13). Animals were killed 2 wk after vascular injury. The experimental carotid arteries were excised, fixed in 4% paraformaldehyde, embedded in paraffin, and serially sectioned at 7 μm for histological staining. Immunostaining was carried out using the anti-p21/p27 antibodies and a Vector Vectastain Elite ABC staining kit (Vector Laboratories, Burlingame, CA) according to the manufacturer's instructions. Pictures were taken using a CCD camera (DP70, Olympus, Melville, NY) attached to a microscope system (BX51, Olympus).

Downloaded from ajpcell.physiology.org on May 27, 2011

Statistical analysis. Values are expressed as means ± SD. The significance of the difference from the control groups was analyzed by Student's *t*-test or one-way analysis of variance (ANOVA) and Bonferroni's method as a post hoc test. A value of $P < 0.05$ was considered statistically significant.

RESULTS

BPS concentration and time dependently induced p21/p27 expression at the transcriptional level. The promoter luciferase-reporter constructs of human p21/p27 were constructed into the pGL3-basic vector, as described previously (21). These constructs were transiently transfected into RASMCs for 24 h, followed by the addition of BPS at concentrations of 0.1~5 μM for 12 h. p21(−2300/+8) luciferase activity increased ~2.0-fold, whereas that of p27(−1358/+132) was enhanced 1.8~2.0-fold by BPS (Fig. 1*A*). The extent of p21/p27 induction by BPS was analyzed at various concentrations and time points. As illustrated in Fig. 1, *B* and *C*, BPS at the concentrations of 0.5~5 μM and at the time points of 6~24 h significantly increased p21/p27 induction, in agreement with data shown in Fig. 1*A*. Moreover, BPS-mediated p21/p27 induction was also confirmed in vivo. Our previous publication (13) demonstrated that giving BPS as a therapeutic treatment for balloon-injured mice decreased the progression of restenosis by about 70% compared with injured mice alone, which was reversed by the addition of 13*S*-hydroxyoctadecaenoic acid (13S-HODE), a PPARδ downregulator (35). Tissue sections from the balloon-injured mice with or without BPS treatment were further subjected to immunohistochemical staining, which showed the apparent induction of p21/p27 with BPS administration (Fig. 1*D*).

Reversal of BPS-modulated inhibition of [^{3}H]thymidine incorporation using p21/p27 antisense oligonucleotides. To further examine the effects of BPS-induced p21/p27 induction on the antiproliferative effects of BPS, [^{3}H]thymidine was incorporated into cells treated with BPS with the addition of the p21/p27 antisense (AS) oligonucleotides. Western blot analysis showed that p21/p27 AS oligonucleotides significantly blocked BPS-mediated p21/p27 induction (Fig. 2*A*). Results in Fig. 2B show that [^{3}H]thymidine incorporation markedly decreased in the sample treated with 1 μM BPS alone. The sample labeled BPS+AS p21 was treated with 40 nM of the p21 AS oligonucleotide (TCCCCAGCCGGTTCTGACAT), which blocked the expression of p21, whereas sample BPS+AS p27 was treated with 40 nM of the p27 AS oligonucleotide (GCAGTTACGCGTCTACACTA), which blocked p27 expression. Treatment of RASMCs with AS p21 or AS p27 alone caused no significant changes in [^{3}H]thymidine incorporation into cells (data not shown). Consequently, pretreatment of RASMCs with AS p21 or AS p27 partially reversed the BPS-induced decrease in [^{3}H]thymidine incorporation. The BPS-induced inhibition of [^{3}H]thymidine incorporation of RASMCs was completely reversed by the combined administration of both AS oligonucleotides to p21/p27 together (Fig. 2*B*). Nevertheless, the sense oligonucleotide of neither p21 (GGACTCGCCTCGCCATCTTA) nor p27 (GACACTCGCACGTTTGACAT) altered the BPS-mediated decrease in DNA synthesis.

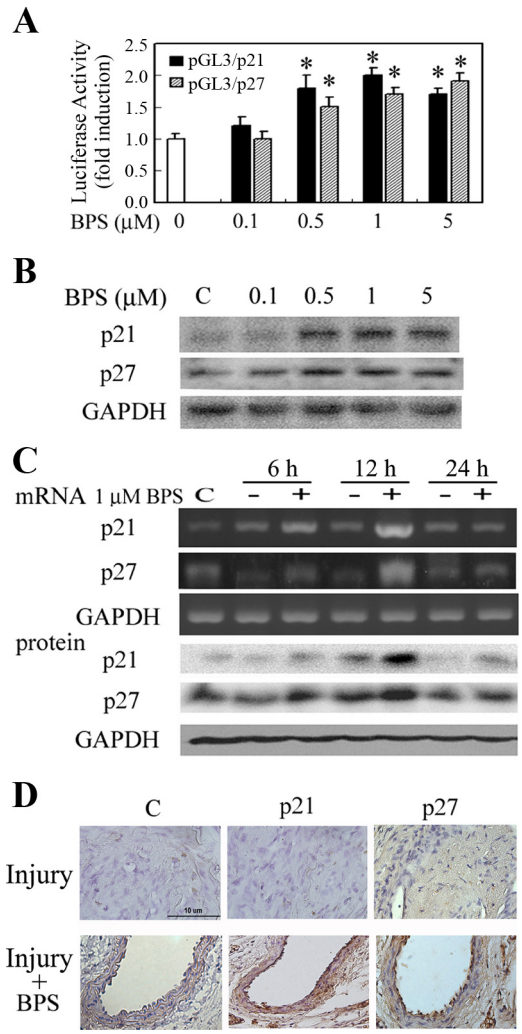

Fig. 1. Transcription regulation of p21 and p27 by beraprost (BPS) in concentration- and time-dependent fashions. *A*: p21 and p27 promoter activities with increasing concentrations of BPS. Rat aortic smooth muscle cells (RASMCs) were transiently transfected with pGL3/p21, p27, and pRL-TK for 24 h, followed by treatment with increasing concentrations of BPS, as described in MATERIALS AND METHODS. Luciferase activities of the reported plasmid were normalized to those of the internal control plasmid and are presented as means ± SD of 4 independent experiments. *$P < 0.05$, significantly different vs. the control group. *B*: concentration-dependent induction of p21/p27 proteins by BPS. Cells were treated with the indicated concentrations of BPS for 12 h, and the expressions of p21/p27 were determined using GAPDH as an internal control. *C*: time-course induction of p21/p27 by BPS. Cells were treated with BPS (1 μM) for 6, 12, and 24 h, and the inductions of p21/p27 were analyzed by RT-PCR and Western blotting. One representative result for 3 separate experiments is shown. *D*: involvement of p21 and p27 in the BPS-mediated prevention of neointimal formation in mice with angioplasty. Two weeks after animals were injured with or without BPS administration ($n = 6$), each injured artery was collected and sectioned for immunohistochemical staining of BPS-induced p21/p27 expression. Representative results are shown.

BPS-mediated increase in CRE-driven luciferase activity depends on PPARδ and CBP but not increased nuclear translocation of CREB. BPS was shown to decrease p27 degradation by a cAMP-dependent pathway (9). The involvement of CREB in BPS-mediated p21/p27 induction in RASMCs was examined. Cell lysates were partitioned into the cytosolic and nuclear fractions at the time points of 10, 30, and 120 min.

Downloaded from ajpcell.physiology.org on May 27, 2011

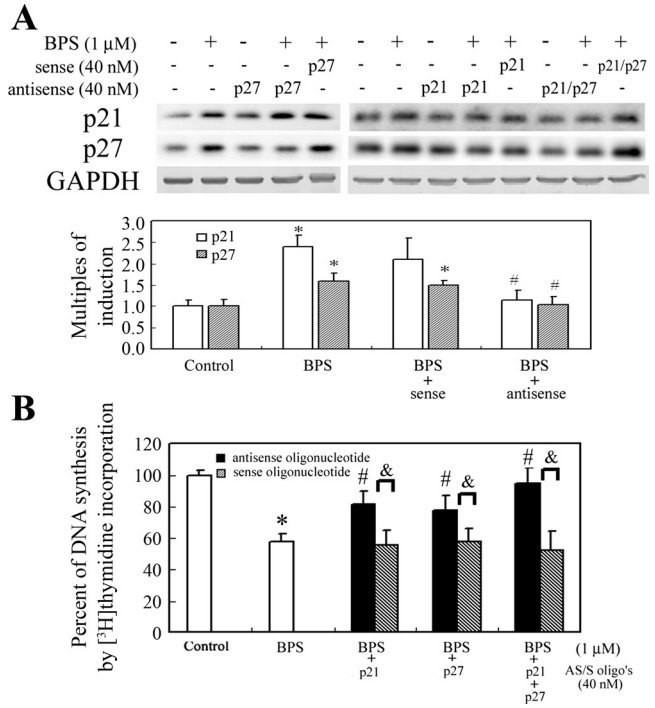

Fig. 2. Reversal of BPS-induced inhibition of thymidine incorporation in RASMCs by p21/p27 antisense (AS) oligonucleotides. *A*: Western blot analysis of p21/p27 blocked by p21/p27 AS oligonucleotides. RASMCs were transfected with scrambled, p21, or p27 AS oligonucleotides at a final concentration up to 40 nM and then treated with 1 μM BPS for an additional 12 h. *B*: effects of p21/p27 AS oligonucleotides on BPS-mediated inhibition of RASMC proliferation by [^{3}H]thymidine incorporation. Six samples were analyzed in each group, and values are presented as means ± SD. *$P < 0.05$ vs. the control. #$P < 0.05$ vs. the BPS-treated group. &$P < 0.05$, sense vs. antisense oligonucleotides.

Results in Fig. 3*A* showed that the total and phosphorylated forms of CREB in the cytosolic and nuclear fractions were not obviously altered upon BPS treatment across the time points examined with respect to the internal controls of GAPDH and histone H3, respectively. To further explore the p21/p27 induction mechanisms by BPS, the pGL2-3CRE and pGL2-3mCRE constructs, described in MATERIALS AND METHODS, were transfected into RASMCs to examine whether BPS increases CRE enhancer activity. Results in Fig. 3*B* show that CRE-driven luciferase activity significantly increased in the range of BPS of 1~5 μM, which was reversed in cells transfected with the pGL2-3mCRE construct. Moreover, BPS was shown by us and others to serve as a PPARδ activator (13, 23, 27), and CBP can be the coactivator for PPAR and CREB to stimulate gene expression (6, 11, 15); thus knockdown of PPARδ and CBP by siRNAs was employed to examine their roles in the increase in CRE-driven luciferase activity induced by BPS. The results in Fig. 3*C* show that cells with PPARδ or CBP knockdown had significantly decreased CRE-driven luciferase activity relative to the control group with 1 μM BPS alone. Nevertheless, the BPS-mediated increase in luciferase was not observed when the consensus binding sites of CREB were mutated or with the combination of cells knocked down with PPARδ or CBP.

Effects of CBP on BPS-mediated p21/p27 induction. Given that PPARδ and CBP are involved in BPS-induced CRE-driven luciferase activity, but not phosphorylation of CREB, alterations in CBP with BPS treatment were investigated. BPS significantly increased nuclear translocation of CBP from 1 to 4 h of treatment (Fig. 4*A*). Additionally, BPS-mediated CBP nuclear translocation was examined by immunofluorescence staining. In control cells, expression of CBP was mainly detected in the cytosol (Fig. 4*A*). After BPS stimulation, CBP protein was significantly translocated into the nucleus. We further used co-IP with an anti-CREB antibody to examine the interplay among the three factors involved in the regulation. Notably, CREB only interacted with CBP (Fig. 4*B*) but not obviously with PPARδ (data not shown).

Next, the effects of CBP on protein levels of p21/p27 and pGL2/rp21- and pGL2/rp27-driven luciferase activity by knocking down CBP in RASMCs were examined. Importantly, based on the in silico analysis using the MatInspector Professor

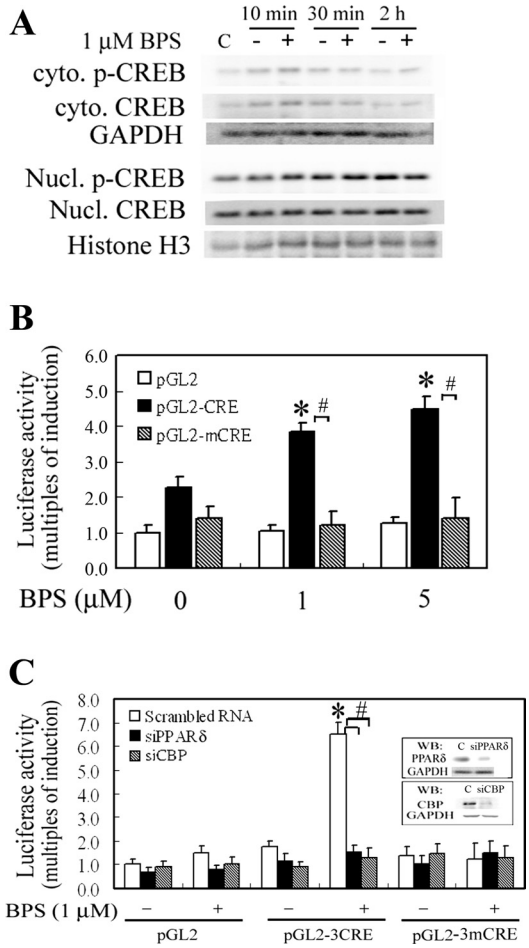

Fig. 3. BPS regulates cAMP-responsive element (CRE) enhancer-driven luciferase activity involved in peroxisome proliferator-activated receptor-δ (PPARδ) and CREB-binding protein (CBP) activation. *A*: Western blot analysis of nuclear-cytosolic partitioning of CREB. Respective weights of the cell lysates were 50 and 30 μg for the cytosolic and nuclear fractions in the analysis. Membranes were respectively probed with anti-GAPDH and anti-histone H3 for the cytosolic and nuclear parts to ensure equal loading in each lane. Representative results of three separate experiments are shown. *B*: BPS increased CRE, but not mCRE, enhancer-driven luciferase activity. The construct is described in MATERIALS AND METHODS. *C*: alleviation of the BPS-mediated increase in CRE enhancer-driven luciferase activity in cells with PPARδ or CBP knockdown. The *insets* in *C* are the Western blot analysis of PPARδ and CBP in cells with/without PPARδ or CBP knockdown. Results are expressed as means ± SD ($n = 4$). Significantly different: *$P < 0.05$ vs. the control; #$P < 0.05$ vs. BPS alone.

Downloaded from ajpcell.physiology.org on May 27, 2011

software, there are putative PPREs next to these putative CRE regions in the p21/p27 promoters. The putative CREs/PPREs from rat p21 (−8671/−8400) and p27 (−1187/−950) promoter regions, designated pGL2/rp21 and pGL2/rp27, were obtained as described in MATERIALS AND METHODS, and we also show their predicted conserved sequences. Rat p21/p27 promoter-driven luciferase activity did not respond to BPS treatment in cells with CBP knockdown in Fig. 4*C*. Similar to the effects of BPS, L-165041, a potent and selective PPARδ ligand, induced p21/p27 promoter activities, whereas these activities were reversed in cells with CBP knockdown. In agreement with the data shown in Fig. 4*C*, the results of Fig. 4*D* showed that BPS-induced p21/p27 protein expression was significantly abolished by knocking down CBP in RASMCs.

Effects of PPARδ on BPS-mediated p21/p27 induction. To further verify the dependence of PPARδ activation in BPS-mediated CBP nuclear translocation and p21/p27 induction, L-165041, a PPARδ ligand, was used as a positive control. Figure 5*A* shows that similar to BPS treatment, activation of PPARδ by L-165041 was concomitant with CBP translocation at 1 h of treatment, whereas the BPS-mediated effects were conversely reversed by GSK0660, a specific PPARδ antagonist (25), and in cells with PPARδ knockdown. Likewise, the elimination of BPS-induced p21/p27 induction by the PPARδ antagonist at 12 h of treatment coincided with the decrease in nuclear translocation of CBP, suggesting the important role of CBP in BPS-mediated p21/p27 induction. Similar to the results of Fig. 5*A*, Fig. 5*B* demonstrates that BPS increased the luciferase activities of pGL2/rp21 and pGL2/rp27, whereas the effects of BPS were partially eliminated in cells transfected with pGL2 vectors containing mutated CRE in the rat p21/p27 promoters, which were further decreased in cells with PPARδ silencing. Furthermore, the effects of BPS on the putative PPREs in the native rat p21 and p27 promoters were evaluated by mutations of the PPREs in these constructs. Mutations of the PPREs in the p21/p27 construct significantly decreased the luciferase activities of the p21/p27 promoter, which in turn decrease further by mutation of CREs in these constructs as demonstrated in Fig. 5*C*, suggesting the important roles of CREs and PPREs in the transcriptional regulation of p21/p27 induction by BPS. Furthermore, to precisely prove the binding of PPARδ to the putative PPREs derived from the p21 and p27 promoter regions, an EMSA was performed using the in vitro-translated PPARδ protein. The results of the EMSA in Fig. 5*D* showed increases in the DNA binding activities of PPARδ, which could be abolished by the competition of a 100-fold molar excess of unlabeled oligonucleotides relative to the radiolabeled probe.

Effects of BPS and PPARδ antagonist on the binding of CREB and CBP to the putative CRE/PPRE of the p21/p27 promoter regions. We further confirmed the effects of BPS or BPS in combination with the PPARδ antagonist GSK0660 on the binding of CREB and CBP to the CRE/PPRE regions of the p21/p27 promoters by a ChIP assay. We performed BPS-induced association of CBP with the CREB-DNA complex by

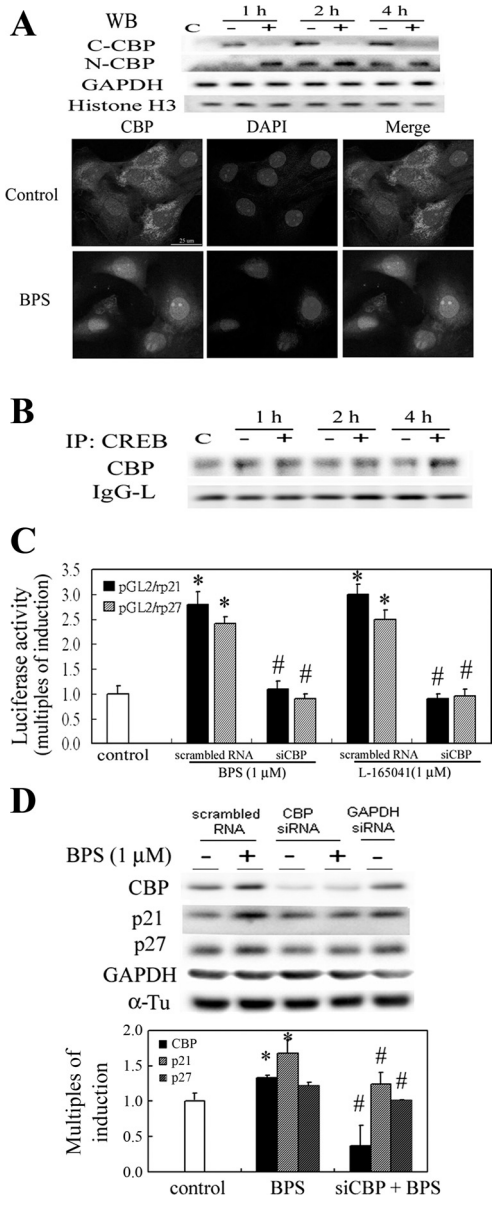

Fig. 4. Evidence of BPS-mediated CBP nuclear translocation and the protein-protein interaction between CREB and CBP. *A*: cells were treated with BPS for 1~4 h and harvested for cytosolic-nuclear partitioning of CBP. Weights of the cell lysates were 50 and 30 μg for the cytosolic and nuclear fractions analyzed, and GAPDH and histone H3 were used as internal controls for these fractions. *A*, *top*: BPS-mediated CBP nuclear translocation on BPS treatment by Western blot analysis. To confirm this phenomenon, immunofluorescence staining of BPS-mediated CBP nuclear translocation in RASMCs was performed. Cells were treated with BPS (1 μM) for 2 h and then immunostained with an anti-CBP antibody followed by incubation with a second antibody conjugated with FITC. *Bottom*: green color represents CBP-positive staining in the cytosol or nuclei. Identical fields stained with CBP were also stained using DAPI to reveal the positions of cell nuclei. Micrographs of representative fields were recorded. *B*: CREB was immunoprecipitated by the anti-CREB antibody and its associated complex was detected with anti-CBP and anti-PPARδ antibodies. Representative results of three independent experiments are shown. *C*: elimination of the BPS-mediated increase in rat p21/p27 promoter-driven luciferase activities in RASMCs with CBP knockdown. *D*: elimination of the BPS-mediated increase in p21/p27 protein levels in RASMCs with CBP knockdown by Western blot analysis. In *C*, a potent PPARδ agonist L-165041 (1 μM) was used as a positive control to determine the effects of BPS and siCBP in the rat p21/p27 promoter-driven luciferase activities. In I, GAPDH small interfering (si)RNA was used as a positive control for knockdown efficiency, and equal loading of each lane is shown by incubating the membrane with an anti-α-tubulin (α-Tu) antibody. Results are expressed as means ± SD ($n = 4$). Significantly different: *$P < 0.05$ vs. the control; #$P < 0.05$ vs. the BPS or L-165041 group.

Downloaded from ajpcell.physiology.org on May 27, 2011

pulling down the CRE/PPRE fragments of the p21/p27 gene promoters using an anti-CREB or anti-CBP antibody and examined whether PPARδ also participates in this ChIP complex formation using an anti-PPARδ antibody. The immunoprecipitated CRE/PPRE fragments were amplified by PCR to examine the binding of CBP, CREB, or PPARδ to the fragments. Figure 6*A* shows that BPS increased CBP and PPARδ recruitment for binding to CRE/PPRE within 1 h by approximately two- to threefold, but not CREB, and that the PPARδ antagonist significantly reduced only CBP and PPARδ, but not CREB, which instead bound to the CRE/PPRE of the p21/p27 promoter to an extent similar to the controls. Together, these results suggest that BPS increased CRE/PPRE-mediated upregulation of p21/p27 by increasing CBP and PPARδ recruitment to CRE/PPRE, which is involved in BPS-mediated PPARδ activation. We further confirmed that PPARδ was part of the ChIP complex by co-IP using an anti-CBP antibody. As shown in Fig. 6*B*, CBP interacted with both CREB and PPARδ, although using anti-CREB and anti-PPARδ antibodies showed only an interaction with CBP but no apparent direct interaction with each other. We also observed that the binding of PPARδ to CBP occurred not only in nuclei but also in the cytosol upon BPS administration by co-IP analysis of cytosolic-nuclear partitioning (data not shown).

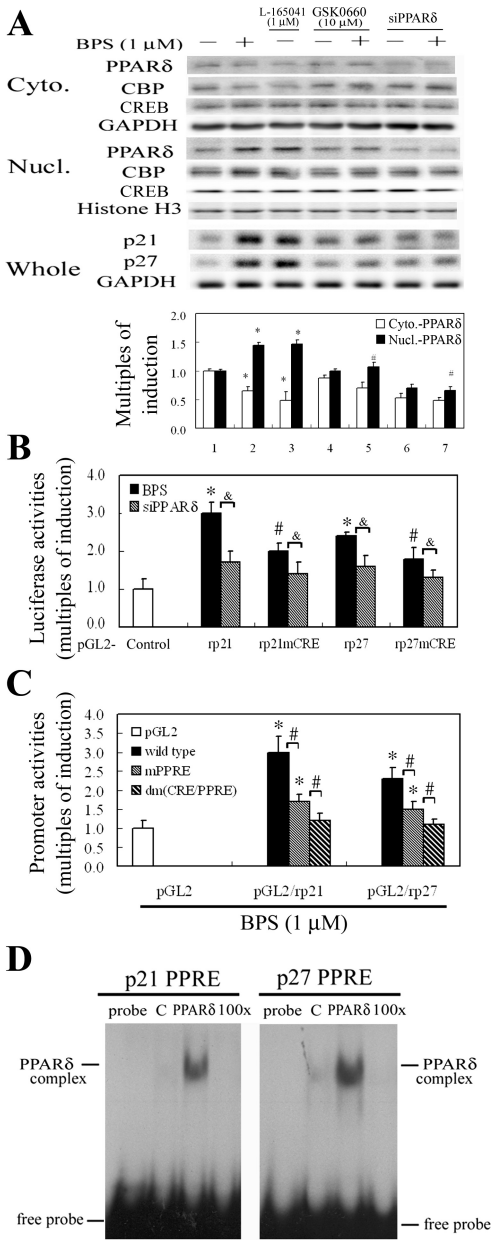

DISCUSSION

In this study, we provide both in vitro and in vivo data to support the roles of p21 and p27 in the antiproliferative action of BPS-mediated PPARδ activation in RASMCs. We also clearly delineate the causal relationship of PPARδ and p21/p27, the protein levels of which were significantly decreased by neutralization of PPARδ activation. p21/p27 induction is involved in the antiproliferative effects of BPS since the addition of p21/p27 AS oligonucleotides significantly reversed the BPS-mediated decrease in DNA synthesis. Additionally, when using BPS for the therapeutic prevention of neointimal formation in mice with angioplasty, significant p21/p27 inductions were observed at injured sites of the carotid artery. Therefore, this might represent another therapeutic mechanism of BPS in protecting against restenosis in vivo; in addition, we previously found that PPARδ-induced iNOS was ascribed to the antiproliferative effects of BPS in an animal model of angioplasty (13).

BPS was shown to prevent the degradation of p27 through cAMP signaling (9); in contrast, we revealed that BPS indeed upregulated involvement of both p21 and p27 in PPARδ activation, which has not been reported before. The results of our investigation demonstrated no apparent difference in pCREB levels in RASMCs treated with BPS by Western blot analysis of cytosol-nuclear partitioning of CREB. Additionally, the specific binding activity of CREB to CRE derived from the p27 promoter region by EMSA was not altered upon BPS administration, though the binding activity declined in the presence of the CREB mutant oligonucleotide (data not shown). On the contrary, CBP is responsible for CRE/PPRE-driven transactivation of p21/p27 in response to BPS administration in RASMCs. The novel finding of significant CBP

Fig. 5. Involvement of PPARδ in increased CBP nuclear translocation in BPS-mediated p21/p27 induction. *A*: elimination of PPARδ on BPS-mediated effects in the partitioning of total cell lysates. Equal loading or transfer was confirmed by incubation with an anti-GAPDH or anti-histone H3 antibody. Representative results of three separate experiments are shown. *B*: effects of BPS on rat-derived putative CRE/PPRE in p21/p27 promoters. Wild types and mutants of p21/p27 CREs were obtained as described in MATERIALS AND METHODS. Cells with or without PPARδ knockdown were transfected with these CRE constructs for 24 h, followed by BPS treatment for 6 h. Luciferase activities of the reported plasmid were normalized to those of the internal control plasmid and are presented as means ± SD of 4 independent experiments. Significantly different: $*P < 0.05$ vs. the control; $\#P < 0.05$ vs. wild type treated with BPS alone; $\&P < 0.05$ vs. BPS alone. *C*: effects of mutation of PPRE and CRE/PPRE on the luciferase activities of rat p21/p27 promoters by BPS. The single mutants or double mutants (dm) of p21' and p27' PPRE or CRE/PPRE in the rat p21/p27 promoter regions were obtained as described in MATERIALS AND METHODS. Results are presented as means ± SD of 4 independent experiments. Significantly different: $*P < 0.05$ vs. the control; $\#P < 0.05$ vs. BPS alone. *D*: EMSA analysis of PPARδ binding activity using in vitro translation of the PPARδ protein. The putative PPREs predicted by MatInspector Professional software were derived from p21 and p27 promoter regions as described in MATERIALS AND METHODS and were used as probes in the EMSA. Representative results of three separate experiments are shown.

Downloaded from ajpcell.physiology.org on May 27, 2011

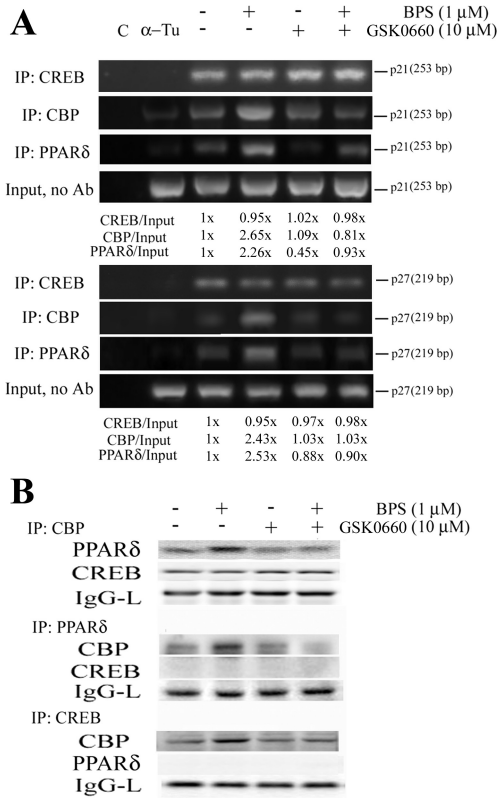

Fig. 6. Antagonized PPARδ activity reduces the association of BPS-induced PPARδ and CBP, but not CREB, with the CRE/PPRE of the p21/p27 promoters. RASMCs were pretreated with a PPARδ antagonist GSK0660 (10 μM) for 1 h followed by 1 μM BPS for 4 h. Cells were harvested and subjected to a chromatin immunoprecipitation (ChIP) assay (*A*) and co-immunoprecipitation (co-IP) (*B*) using anti-PPARδ and anti-CBP antibodies. In *A*, the DNA associated with CREB, CBP, or PPARδ was immunoprecipitated with an anti-CREB, anti-CBP, or anti-PPARδ antibody, and PCR amplification was used to determine the extent of CREB, CBP, and PPARδ association with the CREs of the p21/p27 promoter fragments of 253 and 219 bp, respectively. Distilled water (*C*) and anti-α-tubulin (α-Tu) were respectively used as negative controls for the PCR and the ChIP assays. In *B*, CBP, PPARδ, or CREB was respectively immunoprecipitated with an anti-CBP, -PPARδ, or -CREB antibody, and the associated complex was detected with its respective counterpart antibodies. Representative results of three separate experiments are shown.

nuclear translocation upon BPS treatment is shown in Fig. 4*A*, which has not been addressed before. Interestingly, this process was also dependent on BPS-induced PPARδ activation, as PPARδ siRNA and a PPARδ antagonist (GSK0660) decreased CBP nuclear translocation and thus protein levels of p21/p27, which was further confirmed using a specific PPARδ agonist L-165401. Moreover, chromatin immunoprecipitation with the CBP or CREB antibody confirmed our finding that CBP, but not CREB, plays an essential role in CRE-driven transactivation of p21/p27 by BPS. This result is in accord with a recent study showing that CRE-bound pCREB is insufficient to drive a large amount of CRE-driven gene transcription in the absence of CBP occupancy (3). Interestingly, we proved that novel functional PPREs next to the CREs in the p21/p27 promoter regions are responsible for BPS-mediated CBP nuclear translocation (Fig. 5*C*) and that PPARδ is part of the ChIP complex shown in Fig. 6*A*, which was further confirmed by the co-IP assay using an anti-CBP antibody in Fig. 6*B*.

However, a number of studies also demonstrated controversial roles of cAMP in SMC proliferation/migration and vascular remodeling. Recently, it was shown that BPS increases inducible cAMP early repressor, thereby inhibiting growth of vascular SMCs (20). Additionally, exchange protein activated by cAMP (Epac 1) was identified as a new target molecule of the cAMP signal, which is independent of cAMP-mediated PKA activation. Epac1 is upregulated during neointimal formation and promotes vascular SMC migration (31). Whether BPS eliminates EPAC upregulation, thereby inhibiting SMC proliferation and migration or whether inducible cAMP early repressor is involved in modulating the activity of CRE/CREB in our setting requires further investigation.

The correlation and molecular mechanisms of PPARδ activation and p21/p27 induction have not yet been defined. The novel finding of this study is that BPS-mediated PPARδ activation and the subsequent CBP nuclear translocation are essential to increase CRE/PPRE enhancer activity with the concomitant downstream transactivation of p21/p27, which contributes to the antiproliferative effect of BPS in RASMCs. These results also agree with the findings that the loss of CBP causes T cell lymphomagenesis in synergy with p27 insufficiency (3). Moreover, in agreement with PPARδ dependency on BPS-mediated p21/p27 induction, one of the PPAR family members, PPARγ, was shown to retard cell proliferation through an increase in the cyclin-dependent inhibitor p21 (14). Interestingly, we also showed that BPS increased the luciferase activities of human p21 and p27 promoters in RASMCs as shown in Fig. 1*A*, suggesting that the likelihood of BPS-mediated p21/p27 induction occurs in humans via a PPARδ-dependent mechanism.

In the present study, we examined the potential effects of PPARδ induced by BPS on the inhibition of vascular SMC proliferation. Apparently, the present finding is contradictory to a recent report showing that PPARδ induced by PDGF or by carotid balloon injury promoted cell proliferation in RASMCs (33). The discrepancy of PPARδ on RASMC proliferation might be attributed to whether it is properly ligand bonded (i.e., BPS, a PGI_2 agonist, a natural ligand of PPARδ) or what its inducers are. However, this is speculation and requires further investigation.

From all of these findings, we suggest that BPS-induced PPARδ activation retards cell proliferation through CRE/PPRE-driven p21/p27 induction, which is highly dependent on CBP nuclear translocation in RASMCs. In this study, the results of PPARδ-mediated p21/p27 induction complemented our previous finding of PPARδ-mediated iNOS induction by BPS, both of which exert antiproliferative actions of BPS in RASMCs. Although eNOS and iNOS gene transfers to vascular SMCs were shown to inhibit cell proliferation via upregulation of p21/p27, whether increased iNOS by BPS-mediated PPARδ activation has any synergistic effect on the induction of p21/p27 remains to be further investigated (24, 32).

In summary, our results taken together with those reported in the literature suggest a model in which BPS promotes PPARδ activity and thereby the binding of PPARδ and CBP to the CREB-DNA complex, resulting in increased p21/p27 induction. Together, these effects result in an antiproliferative effect in RASMCs. Herein, we demonstrated the potential effects of PPARδ induced by BPS on inhibiting RASMC proliferation and its implications in preventing restenosis in mice with

Downloaded from ajpcell.physiology.org on May 27, 2011

angioplasty. Identifying the proteins, including PPARδ, p21, and p27, responsible for the antiproliferation of RASMCs by BPS will provide an important molecular basis for the design of new therapeutic strategies to treat atherosclerosis, restenosis, and stroke.

GRANTS

This study was supported by grants (NSC95-2320-B-038-018-MY2) from the National Science Council, Taiwan and (97TMU-WFH-08) Taipei Medical University-Wan Fang Hospital.

REFERENCES

1. **Evans RM, Barish GD, Wang YX.** PPARs and the complex journey to obesity. *Nat Med* 10: 355–361, 2004.
2. **Fisher-Dzoga K, Jones RM, Vesselinovitch D, Wissler RW.** Ultrastructural and immunohistochemical studies of primary cultures of aortic medial cells. *Exp Mol Pathol* 18: 162–176, 1973.
3. **Geiger TR, Sharma N, Kim YM, Nyborg JK.** The human T-cell leukemia virus type 1 tax protein confers CBP/p300 recruitment and transcriptional activation properties to phosphorylated CREB. *Mol Cell Biol* 28: 1383–1392, 2008.
4. **Goodman RH, Smolik S.** CBP/p300 in cell growth, transformation, and development. *Genes Develop* 14: 1553–1577, 2000.
5. **Graham TL, Mookherjee C, Suckling KE, Palmer CN, Patel L.** The PPARdelta agonist GW0742X reduces atherosclerosis in LDLR(-/-) mice. *Atherosclerosis* 181: 29–37, 2005.
6. **Grossman SR.** p300/CBP/p53 interaction and regulation of the p53 response. *Eur J Biochem* 268: 2773–2778, 2001.
7. **Hertz R, Berman I, Keppler D, and Bar-Tana J.** Activation of gene transcription by prostacyclin analogues is mediated by the peroxisome-proliferators-activated receptor (PPAR). *Eur J Biochem* 235: 242–247, 1996.
8. **Hiatt WR.** Medical treatment of peripheral arterial disease and claudication. *N Engl J Med* 344: 1608–1621, 2001.
9. **Ii M, Hoshiga M, Fukui R, Negoro N, Nakakoji T, Nishiguchi F, Kohbayashi E, Ishihara T, Hanafusa T.** Beraprost sodium regulates cell cycle in vascular smooth muscle cells through cAMP signaling by preventing down-regulation of p27(Kip1). *Cardiovasc Res* 52: 500–508, 2001.
10. **Jain M, He Q, Lee WS, Kashiki S, Foster LC, Tsai JC, Lee ME, Haber E.** Role of CD44 in the reaction of vascular smooth muscle cells to arterial wall injury. *J Clin Invest* 97: 596–603, 1996.
11. **Kang-Decker N, Tong C, Boussouar F, Baker DJ, Xu W, Leontovich AA, Taylor WR, Brindle PK, van Deursen JM.** Loss of CBP causes T cell lymphomagenesis in synergy with p27Kip1 insufficiency. *Cancer Cell* 5: 177–189, 2004.
12. **Kim DJ, Murray IA, Burns AM, Gonzalez FJ, Perdew GH, Peters JM.** Peroxisome proliferator-activated receptor-beta/delta inhibits epidermal cell proliferation by down-regulation of kinase activity. *J Biol Chem* 280: 9519–9527, 2005.
13. **Lin H, Lee JL, Hou HH, Chung CP, Hsu SP, Juan SH.** Molecular mechanisms of the antiproliferative effect of beraprost, a prostacyclin agonist, in murine vascular smooth muscle cells. *J Cell Physiol* 214: 434–441, 2008.
14. **Lin Y, Zhu X, McLntee FL, Xiao H, Zhang J, Fu M, Chen YE.** Interferon regulatory factor-1 mediates PPARgamma-induced apoptosis in vascular smooth muscle cells. *Arterioscler Thromb Vasc Biol* 24: 257–263, 2004.
15. **Mochizuki K, Suruga K, Sakaguchi N, Takase S, Goda T.** Major intestinal coactivator p300 strongly activates peroxisome proliferator-activated receptor in intestinal cell line, Caco-2. *Gene* 291: 271–277, 2002.
16. **Nakajima T, Uchida C, Anderson SF, Lee CG, Hurwitz J, Parvin JD, Montminy M.** RNA helicase A mediates association of CBP with RNA polymerase II. *Cell* 90: 1107–1112, 1997.
17. **Narumiya S, Sugimoto Y, Ushikubi F.** Prostanoid receptors: structures, properties, functions. *Physiol Rev* 79: 1193–1226, 1999.
18. **Niwano K, Arai M, Tomaru K, Uchiyama T, Ohyama Y, Kurabayashi M.** Transcriptional stimulation of the eNOS gene by the stable prostacyclin analogue beraprost is mediated through cAMP-responsive element in vascular endothelial cells: close link between PGI2 signal and NO pathways. *Circ Res* 93: 523–530, 2003.
19. **Ogryzko VV, Schiltz RL, Russanova V, Howard BH, Nakatani Y.** The transcriptional coactivators p300 and CBP are histone acetyltransferases. *Cell* 87: 953–959, 1996.
20. **Ohtsubo H, Ichiki T, Miyazaki R, Inanaga K, Imayama I, Hashiguchi Y, Sadoshima J, Sunagawa K.** Inducible cAMP early repressor inhibits growth of vascular smooth muscle cell. *Arterioscler Thromb Vasc Biol* 27: 1549–1555, 2007.
21. **Pang PH, Lin YH, Lee YH, Hou HH, Hsu SP, Juan SH.** Molecular mechanisms of p21 and p27 induction by 3-methylcholanthrene, an aryl-hydrocarbon receptor agonist, involved in antiproliferation of human umbilical vascular endothelial cells. *J Cell Physiol* 215: 161–171, 2008.
22. **Piech-Dumas KM, Best JA, Chen Y, Nagamoto-Combs K, Osterhout CA, Tank AW.** The cAMP responsive element and CREB partially mediate the response of the tyrosine hydroxylase gene to phorbol ester. *J Neurochem* 76: 1376–1385, 2001.
23. **Prescott SM, White RL.** Self-promotion? Intimate connections between APC and prostaglandin H synthase-2. *Cell* 87: 783–786, 1996.
24. **Sato J, Nair K, Hiddinga J, Eberhardt NL, Fitzpatrick LA, Katusic ZS, O'Brien T.** eNOS gene transfer to vascular smooth muscle cells inhibits cell proliferation via upregulation of p27 and p21 and not apoptosis. *Cardiovasc Res* 47: 697–706, 2000.
25. **Shearer BG, Steger DJ, Way JM, Stanley TB, Lobe DC, Grillot DA, Iannone MA, Lazar MA, Willson TM, Billin AN.** Identification and characterization of a selective peroxisome proliferator-activated receptor beta/delta (NR1C2) antagonist. *Mol Endocrinol* 22: 523–529, 2008.
26. **Sherr CJ, Roberts JM.** CDK inhibitors: positive and negative regulators of G1-phase progression. *Genes Develop* 13: 1501–1512, 1999.
27. **Vane JR, Botting RM.** Pharmacodynamic profile of prostacyclin. *Am J Cardiol* 75: 3A–10A, 1995.
28. **Weber AA, Zucker TP, Hasse A, Bonisch D, Wittpoth M, Schror K.** Antimitogenic effects of vasodilatory prostaglandins in coronary artery smooth muscle cells. *Basic Res Cardiol* 93, *Suppl 3*: 54–57, 1998.
29. **Wung BS, Cheng JJ, Hsieh HJ, Shyy YJ, Wang DL.** Cyclic strain-induced monocyte chemotactic protein-1 gene expression in endothelial cells involves reactive oxygen species activation of activator protein 1. *Circ Res* 81: 1–7, 1997.
30. **Xu W, Kasper LH, Lerach S, Jeevan T, Brindle PK.** Individual CREB-target genes dictate usage of distinct cAMP-responsive coactivation mechanisms. *EMBO J* 26: 2890–2903, 2007.
31. **Yokoyama U, Minamisawa S, Quan H, Akaike T, Jin M, Otsu K, Ulucan C, Wang X, Baljinnyam E, Takaoka M, Sata M, Ishikawa Y.** Epac1 is upregulated during neointima formation and promotes vascular smooth muscle cell migration. *Am J Physiol Heart Circ Physiol* 295: H1547–H1555, 2008.
32. **Zeng Q, Ran PX, Chen SC, Liu JS.** The inhibitory mechanism of nitri-oxide synthase gene transfection on hypoxia-induced proliferation of rat pulmonary arterial smooth muscle cells. *Zhonghua Jie He He Hu Xi Za Zhi* 26: 358–361, 2003.
33. **Zhang J, Fu M, Zhu X, Xiao Y, Mou Y, Zheng H, Akinbami MA, Wang Q, Chen YE.** Peroxisome proliferator-activated receptor delta is up-regulated during vascular lesion formation and promotes postconfluent cell proliferation in vascular smooth muscle cells. *J Biol Chem* 277: 11505–11512, 2002.
34. **Zhang X, Odom DT, Koo SH, Conkright MD, Canettieri G, Best J, Chen H, Jenner R, Herbolsheimer E, Jacobsen E, Kadam S, Ecker JR, Emerson B, Hogenesch JB, Unterman T, Young RA, Montminy M.** Genome-wide analysis of cAMP-response element binding protein occupancy, phosphorylation, and target gene activation in human tissues. *Proc Natl Acad Sci USA* 102: 4459–4464, 2005.
35. **Zuo X, Wu Y, Morris JS, Stimmel JB, Leesnitzer LM, Fischer SM, Lippman SM, Shureiqi I.** Oxidative metabolism of linoleic acid modulates PPAR-beta/delta suppression of PPAR-gamma activity. *Oncogene* 25: 1225–1241, 2006.

Downloaded from ajpcell.physiology.org on May 27, 2011